African Journal of Advanced Pure and Applied Sciences (AJAPAS)
Online ISSN: 2957-644X
Volume 4, Issue 3, 2025
Page No: 393-402
Website: https://aaasjournals.com/index.php/ajapas/index
ISI 2025: 1.126 SJIFactor 2024: 6.752 معامل التأثير العربي: 1.62

Coating and Hardening of Plastic Recycling Machine Blades Using Flux–Cored Arc Welding (FCAW) Process

Murad Ayad Debeski [1], Maryam Mohamed Morghem [*2], Khaled Suliman Elgomati [3]
[1,2,3] Libyan Advanced Occupational Center for Welding Technologies, Tajora, Libya

تكسية وتصليب شفرات آلة إعادة تدوير البلاستيك باستخدام عملية اللحام بالسلك المجوف *FCAW*

مراد عياد الدبسكي [1]، مريم محمد مرغم [*2] ، خالد سليمان القماطي [3]
[3،2،1] المركز الليبي المهني المتقدم لتقنيات اللحام، تاجوراء، ليبيا

[*]Corresponding author: mariammorgham@gmail.com

Received: June 29, 2025	Accepted: August 22, 2025	Published: September 02, 2025

Abstract:
Plastic pollution presents a critical global challenge, largely driven by inadequate waste management and recycling initiatives. Plastic shredders play a pivotal role in addressing this issue by fragmenting plastic waste into manageable pieces for reuse. This study focuses on enhancing the mechanical characteristics of low-carbon steel blades used in plastic shredders through utilizing wire welding techniques. Specifically, the research examines the microstructural and microhardness properties of low-carbon steel blades enhanced through an arc with a flux core arc E71T-GS filler electrodes, a single buttering layer of hard-facing material is applied to improve wear resistance and durability.
Metallurgical analysis, using optical microscopy and micro-Vickers hardness testing, revealed the presence of martensitic and tempered needle-like structures in the heat-affected zone. These features are influenced by specific current and voltage parameters during welding. Comparative analysis was conducted with blades sourced from two other companies (denoted as M and U) to establish performance benchmarks.
The hard-facing layer, enriched with $(Fe,Cr)_7C_3$ carbides embedded in a martensite-austenite matrix, demonstrated significantly enhanced hardness and wear resistance. Vickers hardness testing confirmed superior microhardness in the hard-facing layer, with a gradual and cohesive transition to the softer steel substrate. This optimized microstructure allows the blades to endure high-stress conditions while maintaining durability and toughness. These findings underscore the potential of molten wire welding to significantly enhance the performance and lifespan of shredder blades, providing valuable insights for the design of more efficient plastic waste management systems.

Keywords: Plastic Shredder, Flux Cored Welding Process, Metallurgical analysis.

الملخص
يمثل تلوث البلاستيك تحديًا عالميًا بالغ الأهمية، ويرجع ذلك إلى حد كبير من مبادرات إدارة النفايات وإعادة التدوير الغير كافية. تلعب آلات تقطيع البلاستيك دورًا محوريًا في معالجة هذه المشكلة من خلال تفتيت النفايات البلاستيكية إلى قطع قابلة للإدارة لإعادة الاستخدام. تركز هذه الدراسة على تحسين الخصائص الميكانيكية لشفرات الفولاذ منخفض الكربون المستخدمة في آلات تقطيع البلاستيك من خلال الاستفادة من تقنيات اللحام بالأسلاك. على وجه التحديد، يدرس البحث خصائص البنية الدقيقة والصلابة الدقيقة لشفرات الفولاذ منخفض الكربون المعززة من خلال تكسية الشفرات بطبقة صلبة لتحسين مقاومة التآكل والمتانة باستخدام تقنية اللحام بالقوس الكهربائي بالسلك المجوف FCAW بسلك تغذية E71T-.GS بقطر 1مم.
كشف التحليل المعدني، بإستخدام المجهر الضوئي واختبار صلابة فيكرز الدقيقة، عن وجود هياكل مارتنسيتية وإبرية مخففة في المنطقة المتأثرة بالحرارة. تتأثر هذه الميزات بمتغيرات التيار والجهد المحددة أثناء اللحام. تم إجراء تحليل مقارن باستخدام شفرات تم الحصول عليها من شركتين مختلفتين يشار إليهما باسم M و U لتحديد معايير الأداء. أظهرت الطبقة الصلبة المغطاة، المخصبة بكربيدات $(Fe,Cr)_7C_3$ المضمّنة في مصفوفة مارتنسيت-أوستينيت، صلابة ومقاومة تآكل محسّنة بشكل

كبير. أكّد اختبار صلابة فيكرز على صلابة دقيقة فائقة في الطبقة الصلبة المغطاة، مع انتقال تدريجي ومتماسك إلى الطبقة الأساسية الفولاذية الأكثر ليونة. تسمح هذه البنية الدقيقة المحسنة للشفرات بتحمل ظروف الإجهاد العالية مع الحفاظ على المتانة والصلابة. تؤكد هذه النتائج على إمكانات اللحام بالأسلاك المنصهرة لتعزيز أداء وإطالة عمر شفرات التقطيع بشكل كبير، مما يوفر رؤى قيمة لتصميم أنظمة إدارة النفايات البلاستيكية الأكثر كفاءة.

الكلمات المفتاحية: آلة فرم البلاستيك، اللحام بالقوس الكهربائي بالسلك المجوف FCAW ، التحليل المعدني.

Introduction

Since the 1950s, with the advent of mass production of plastic, this material has become an essential part of our daily lives. With growing populations, improved living standards, and technological advancements, reliance on plastic has steadily increased [1]. This is due to its obvious advantages: it is cheap, lightweight, and easy to shape. Thanks to these versatile properties, plastic have been able to replace many traditional materials such as metal, wood, and leather [2]. Today, plastic is widely used in food and beverage packaging, the textile industry, automotive parts, industrial processes, and in the medical field, such as surgical instruments, intravenous solutions, and medicine containers [3]. However, this widespread use has brought with it serious environmental problems that have burdened terrestrial and marine ecosystems [4]. According to a 2018 report by the United Nations Environment Programmed (UNEP), only 9% of the nine billion tons of plastic produced globally have been recycled, with most of it ending up in landfills, landfills, or the environment [5]. Recycling is mostly carried out through centralized systems [6], but this system is a major reason for low recycling rates due to the difficulty of collecting, sorting, shredding, and transporting plastic waste. In developing countries such as Malaysia, waste management infrastructure remains insufficient to support effective recycling programs [7]. Furthermore, recycling requires significant financial investments and operational resources [8]. Despite these challenges, the importance of recycling has not gone unnoticed, as some independent companies, NGOs, and local communities have launched initiatives to encourage recycling as much as possible. One example is the Australian non-profit organization Sea Communities, which established a recycling center serving the residents of the village of Les, located on the northern coast of Bali, Indonesia, to address the plastic waste problem there. [9]. Central to the plastic recycling process is the shredder machine, which cuts plastic waste into manageable pieces for easier processing and conversion into new products. To address minor to moderate-scale recycling needs, "Cutting-edge shredding machines have been designed to enhance efficiency and performance One particularly promising method to enhance the performance of these machines is hard-facing, which provides a cost-effective solution by creating a durable clad layer that offers wear resistance, heat resistance, and corrosion resistance. [10]. among all the existing techniques, this research examines the worldwide challenge of plastic pollution stemming from insufficient waste management and recycling initiatives, with an emphasis on improving the efficacy of plastic shredders. These devices break down plastic waste into smaller fragments for recycling into valuable products, and their efficiency is significantly affected by the design and materials of essential components such as shafts and blades. Hard-facing has emerged as a highly effective surface engineering strategy owing to its exceptional cost-efficiency, the superior hardness of the deposited layer, robust interfacial bonding strength, and substantially reduced residual stress [11,12–14]. The microstructural and functional attributes of the surfacing layer are predominantly governed by the metallurgical characteristics and alloying composition of the surfacing electrode. For instance, the deployment of a high-manganese steel surfacing electrode enables the synthesis of a fully austenitic layer distinguished by its pronounced work-hardening capability, enhanced fracture toughness, and excellent wear resistance. [15]. Based on this understanding, the quality of welded joints can be significantly enhanced by precise control of welding process temperatures, including preheating, inter-pass temperature, and cooling rate [16–19]. Preheating of both the base and filler materials prior to welding effectively mitigates various contaminants such as moisture, entrapped gases, and hydrogen, while simultaneously moderating the cooling rate and reducing shrinkage-induced stresses, thereby minimizing preheating-related defect. Flux cored welding is a common technique used to fabricate shredder blades. The microstructure of these welded blades is crucial for understanding their strength, durability, and performance. This study will explore the key aspects of the martensite microstructure in flux cored welded blades.(Lee et al)[20.] In this study, we will explore the metallurgical characterization of hard surfacing applied to low-carbon steel blades using automatic flux-cored arc welding techniques. The research will focus on understanding the microstructure of these welded blades, particularly the martensitic structure resulting from the welding process, and examine how variations in the composition of the filler electrode, particularly increased chromium content, can enhance the strength and toughness of the welds. Ultimately, addressing plastic waste through improved recycling methods is essential for developing countries to achieve environmental sustainability and provide job opportunities. This research aims to contribute to those efforts by enhancing the efficiency of plastic shredders and advancing the quality of their components.

Material and methods.

For the base metal, the (AISI 1045) with dimensions of (40mm×30mm×15mm) was utilized for the experimental investigation. The spectrometric evaluation of both the specimen and the welding metal was conducted using a Spectrometer Machine (OPT 9800-Floor model spectrometer) to ascertain the chemical composition of the materials prior to and subsequent to welding, as detailed in Table 1 and Table 4 respectively. The surface of the specimen was subjected to polishing to eliminate any rust, while the filler material employed was E71T-GS flux-cored wire, possessing a diameter of 1.00mm, with its chemical composition delineated in Table 2, and its mechanical properties illustrated in Table 3. Each specimen was characterized through microstructural analysis. The following methodology was employed: samples were sectioned using Electrical Discharge Machining (EDM) owing to the considerable hardness affiliated with the hard-facing material, followed by polishing and etching, as well as macro and microscopic examination utilizing an optical microscope, and hardness testing. The samples were subsequently prepared for grinding utilizing a systematic approach involving 120, 220, 320, 500, and 1000 grit sandpaper, with multiple polishing stages conducted post-grinding, which included the application of diamond paste of 6 µm, culminating with a final polish of 1 µm. For the etching process, an initial solution of Nital 2% (comprising 98ml of alcohol and 2ml of nitric acid) was employed to contrast the substrate for 10 seconds; thereafter, following the preparation of the samples, a metallographic examination was executed with a Zeiss microscope. Micrographs were captured at magnifications of 50x, 100x, 200x, and 500x**.**

.

Table1: The Chemical Composition of Base Metal.

Element	C%	Si %	Mn %	P%	S %	Cr %	Ni %	Mo %	Al %	Cu %	Co %	Ti %	Nb %	V %
AVE.	0.347	0.22	1.072	0.017	.029	.015	.023	.02	.04	.048	.006	.050	.002	.009

Table 2: Typical Filler Wire Chemistry in weight percent (wt %).(Aws A5.20&ASMESFA)**.**

Element	C%	Si%	Mn%	P%	S%	Cr%	Ni%	M%	Al%	Cu%	Nb%	V%
AVE.	0.12	0.9	1.75	0.03	0.003	0.20	0.50	0.3	.04	0.35	.050	.008

Table 3: Mechanical characteristics of Electrode Wire.

Shielding Gas	CO2	75Ar/25%CO2	AWS Requirements	Application
Tensile resistance (PSi)	84-87,000	89-93,000	70-95,000PSi	This electrode is designed for single and multiple pass welding, also used for welding in all position.
Yield Strength (Psi)	75-777,000	81-83.000	58.000PSi	
Elongation % in 2"	31,1%	30.8%	22%	
Charpy V-notch ft-lbs	79-81	64-65	20	

3.2. Welding Procedure. Experimental procedures were conducted utilizing an E71T-GS electrode in accordance with the AWS A5.20 specifications; this particular wire is employed for the coating of steel components, thereby enhancing their wear and impact resistance properties. The distance from the nozzle to the workpiece was rigorously maintained at 12 mm, with the torch consistently oriented at an angle of 5 degrees. Welding operations were executed in a single pass across the weld plate, as depicted in Figures 2(a) and 2(b). The Flux-Cored Arc Welding (FCAW) technique was utilized in hard-facing mode to maximize the efficient transfer of electrode material onto the substrate, as illustrated in Figures 1a and 1b. The visual representation displays a flat metallic specimen upon which an electric arc welding bead has been deposited utilizing a metal electrode. The weld bead exhibits relatively uniform ripple patterns, signifying a stable feed rate and meticulously controlled hand movement throughout the welding procedure. A number of slag deposits and oxidation residues are observable on the surface surrounding the weld region. Furthermore, the metallic section features an irregularly shaped aperture, presumably resulting from a thermal cutting process or a pre-existing mechanical defect. The specimen is situated on a perforated metal worktable and secured with an electrical grounding clamp to ensure current stability during the welding operation. Prior investigations, such as those conducted by Zhang et al. [21], have examined the impacts of varying flux core compositions on weld bead geometry and mechanical properties. In a similar vein, Chen et al. [22] scrutinized the effects of welding parameters on weld quality. FCAW encompasses the fusion of a flux-cored wire metal and/or a base metal, characterized by a welding heat input typically ranging from 30 to 40 kJ/cm, as indicated by Yan et al. [23]. Consequently, the present study envisions the application of a hard-facing steel consumable wire in conjunction with arc additive manufacturing, facilitating the fabrication of single or multi-material components with enhanced wear resistance. Future endeavors aim to utilize a flux-cored wire, coupled with its hard-facing characteristics, to deposit fully dense components of this material or to coat parts produced through conventional manufacturing and WAAM processes. Therefore, this metal will be examined alongside metal, specifically low carbon steel, known for its high ductility and low hardness, to assess compatibility. Structural steel (as the base metal) sourced from local manufacturers was processed into a rectangular specimen of dimensions (3 cm × 4 cm × 1.5 cm). The microstructure of this specimen reveals the presence of ferrite and pearlite, as depicted in Figure 4a.

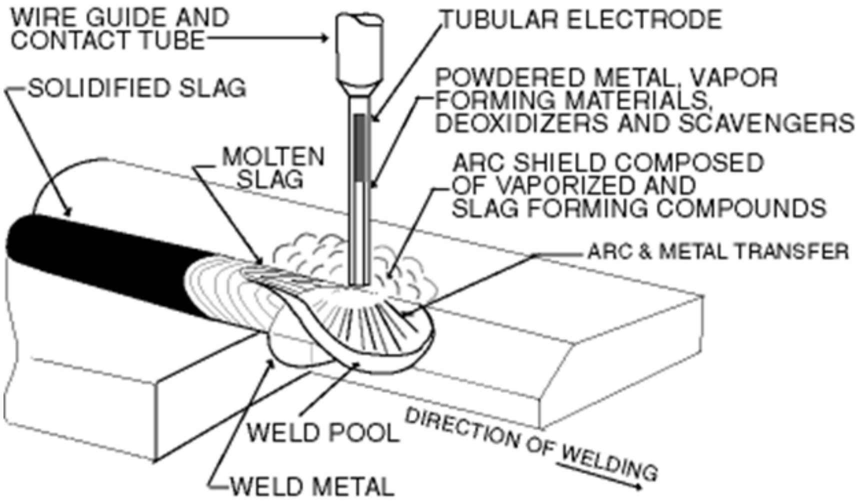

Figure1a: schematic of flux cored machine [22].

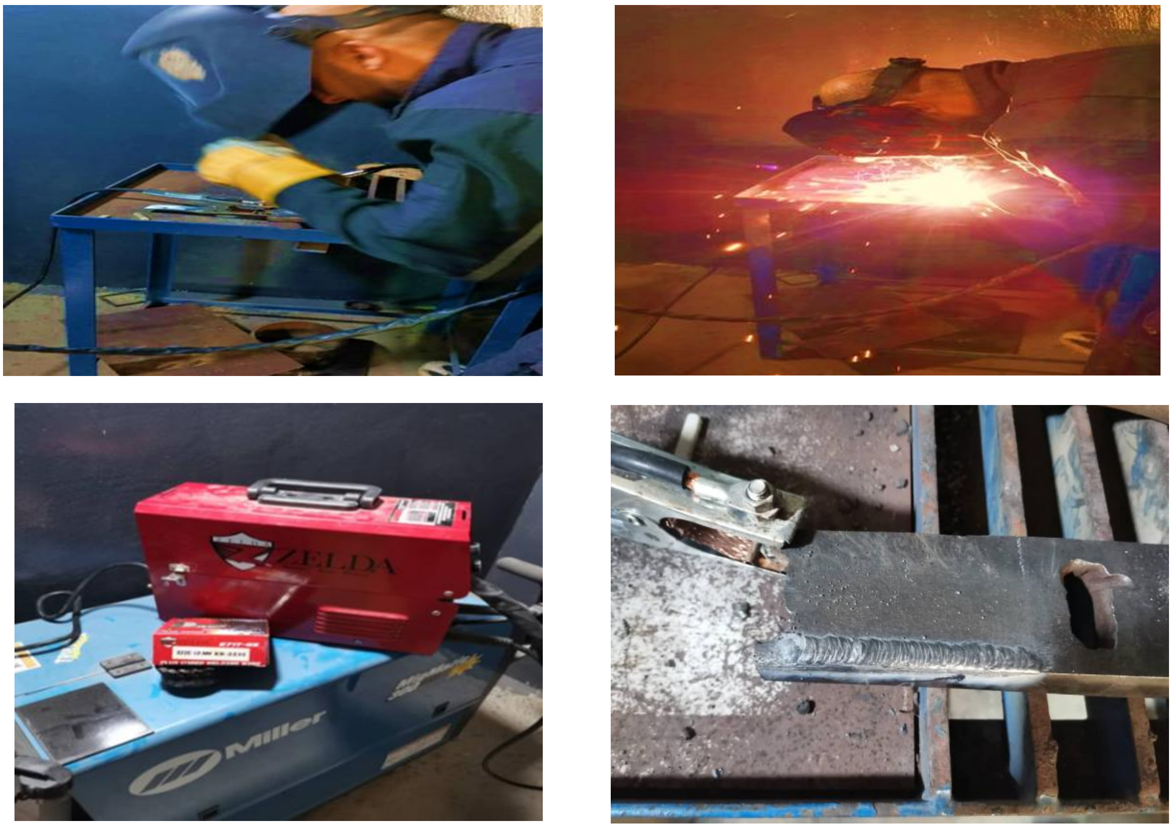

Figure 2a: Shows the Experimental Set up. **2b:** The image shows a flat metallic specimen on which an electric arc welding bead has been deposited using a metal electrode.

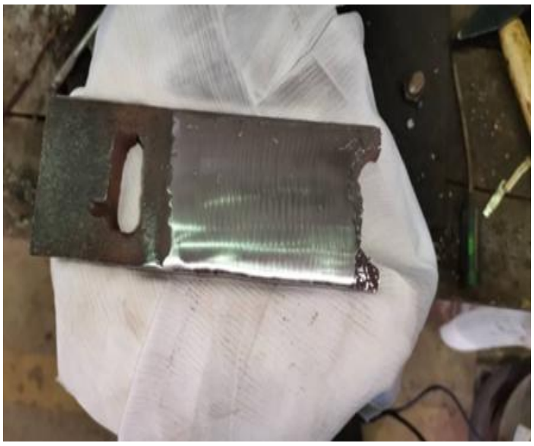

Figure 2c: Sample during Welding. **Figure 2d:** Sample after Welding.

3-3 Evaluation of mechanical charateristics.
Vickers microhardness testing was conducted on different areas of the wall including the bottom, middle bottom, middle top, and the top (see Figure .3), utilizing a Buehler Micromet hardness test machine at a load of 1kg and the loading time of 10sec.

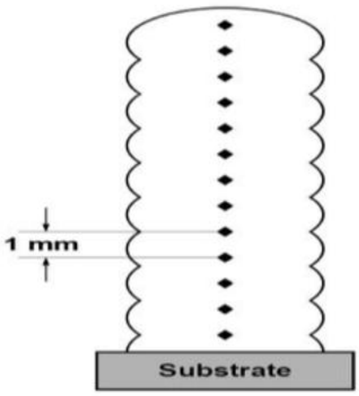

Figure 3: Schematic of Hardness test, vertical measurement points.

4. Results and Discussion
4.1. Microstructure Analysis
Figure 4(a) Shows the typical microstructure of the base metal, which consist of primary ferrite (white) and pearlite (black colonies) but in figure 4(b), the microstructure of(A) specimen (welded specimen) showed an austenitic phase, with a small dendritic structure at the grain boundaries, for the hard-facing zone, the microstructure of specimen clearly showed a martensitic matrix with probably some small austenitic fields at the grain boundaries .The dendritic structure (brighten) was denotes as chromium carbides.
The difference in chemical analyses (as shown in tables 1 and 4) obviously impacts the structure at the micro level in addition to the mechanical characteristics at the macro level. Thus, the microstructures of all materials were examined. Figure 8 shows the microstructure of sample (A) at 100x magnification. Because of its martensitic structure, it can be used for hard-facings that are resistant to impact, compression, and slight abrasion wear[25].
The chemical constituents of the wire For E71-T flux-cored play a critical role in shaping the weld's microstructure helps reduce the promotes the nucleation and growth of proeutectoid ferrite (PF) and while significantly retarding the austenite transformation kinetic. E71T-1 wires contain optimized levels of manganese (Mn) and silicon (Si), which enhance microstructure refinement, increase acicular ferrite content, and improve overall weld performance. These electrodes are suitable for single or multi-pass welding, promoting structures like acicular ferrite or bainite. Acicular ferrite forms via intergranular nucleation on nonmetallic inclusions, while bainite nucleates at austenite grain boundaries. Side lath ferrite, a form of Widmanstätten structure, arises from high welding heat input and rapid air cooling, which can degrade joint performance. It forms at a lower temperature than grain boundary ferrite but belongs to the proeutectoid ferrite family.

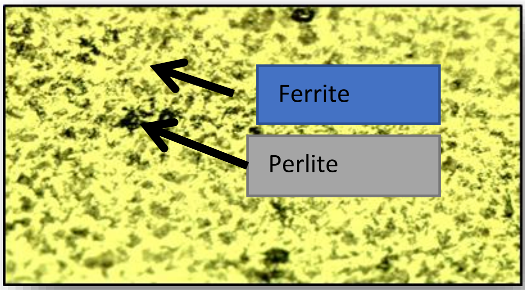

Figure 4a: Microstructure of base metal with Mag.50

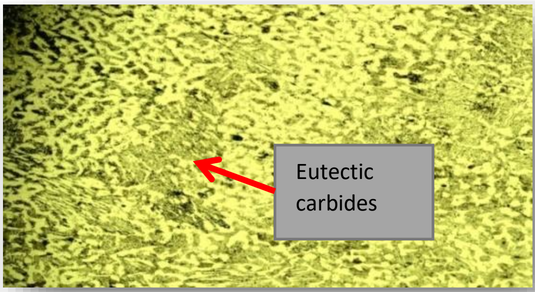

Figure 4b: Microstructure of A specimen with Mag.100x

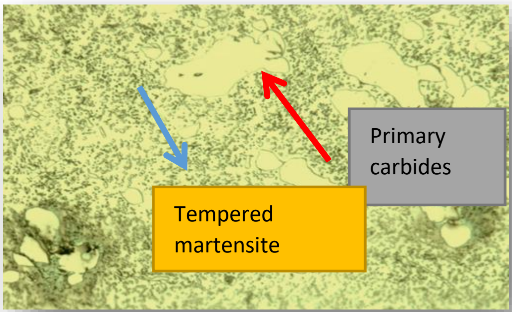

Figure5: Microstructure of M specimen with Mag.100

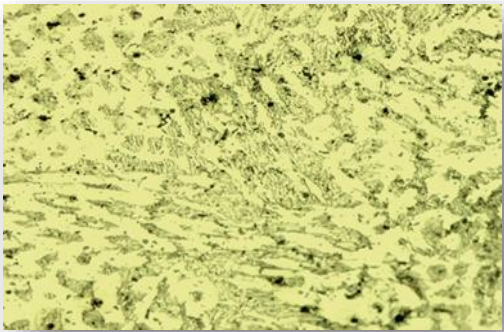

Figur6: Microstructure of (M) specimen with mag.50x

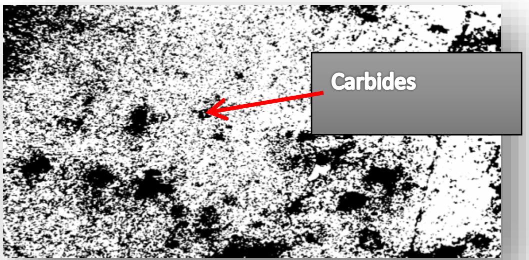

Figure 7: Microstructure of U Sample threshold 50x

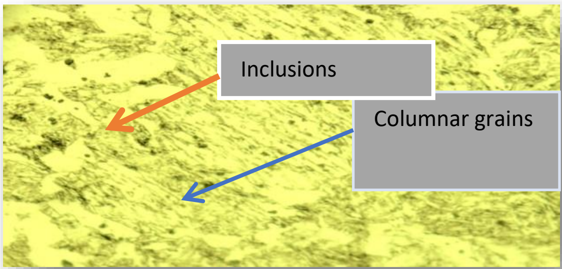

Figure 8: Microstructure of A sample with mag. 100x

Figure (5.7), display chromium carbides were dispersed at random but did not build up. By showing that the hardness and wear properties of the weld metal are uniformly displayed to the structure, this homogeneous distribution offers a significant advantage. Although this sample has a martensitic structure, the carbides are more easily seen, which makes it appropriate for impact and pressure stress situations. However, only grinding can machine the weld deposit.

It is evident from Figure 5 that the microstructure has a uniform distribution of increasing chromium carbides. In comparison to the sample before (U), it is noted that the grains' chromium carbide density has increased. The cause for the variation in the hardness values between samples number (M) and (U) is this rise in the density of chromium carbide within the grains. Idlers, digging buckets, digging teeth, ploughshares, mixing wings, and conveyor screws are among the parts formed of carbon steel, cast steel, or Mn-steel that are subject to grinding wear and are sprayed with the high chromium carbides alloyed hard-facing sample [26].

Figure 9 illustrates that the increased carbon content in the metal matrix of sample (M) promotes the formation of graphite. Although this higher carbon level shows only a slight effect on hardness, it leads to a clear improvement in wear resistance compared to sample (A). These findings highlight the potential of such microstructural modifications for producing durable claddings in components exposed to moderate impact and severe abrasive conditions, including sand pumps, mixer blades, digger teeth, conveyor screws, and scraper blade [27].

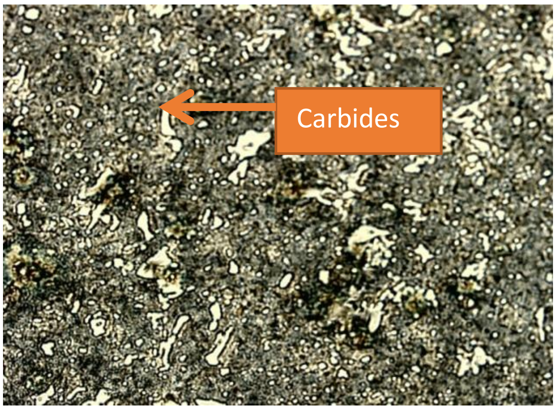

Figure 9: Microstructure of M sample with mag. 20x

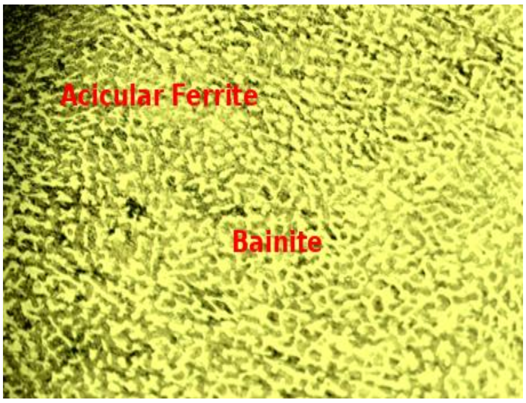

figure 10: Microstructure of A sample (20x)

.

In figure 10. Acicular Ferrite (Highlighted in the majority of the image): These are fine needle-like structures dispersed across the weld microstructure. They appear darker or in contrast to other phases and form within the grains on nonmetallic inclusions. Bainite (Possible regions near grain boundaries): Appearing slightly coarser than acicular ferrite, bainite forms along the grain boundaries and contributes to strength. It may look darker in localized areas compared to acicular ferrite.

Proeutectoid Ferrite (Potential residual traces): These might appear as lighter, polygonal shapes at the grain boundaries. However, E71-T electrodes are designed to suppress excessive proeutectoid ferrite formation. Nonmetallic Inclusions (Subtle specks or clusters). These serve as acicular ferrite nucleation sites and are essential for the formation of this desired microstructure.

Table 4: The Chemical Constituents of sample after welding.

Element	C%	Si%	Mn%	P%	S%	Cr%	Ni%	Mo%	Al%	Cu%	Co%	Ti%	Nb%	V%
AVE.	0.25	0.359	0.773	.012	.005	.026	.013	.129	1.862	.025	.004	.019	.008	.006

Table 5: Chemical Constituents of M Sample.

Element	C%	Si%	Mn	P	S	Cr	Ni	Mo	Al	Cu	Co	Ti	Nb	V	W
Average	2.231	.614	.334	.030	.006	11.588	.145	.077	.112	.055	.032	.023	.006	.098	.07

Table 6: Chemical Constituents of U Sample.

Element	C%	Si%	Mn	P	S	Cr	Ni	Mo	Al	Cu	Co	Ti	Nb	V	W
Average	**.405**	**.262**	**.687**	**.0110**	**.015**	**1.858**	**.043**	**.446**	**.986**	**.032**	**.053**	**.008**	**.002**	**.009**	**.032**

4.2. Micro hardness Results.

Figures (11–14) illustrate the variation in Vickers microhardness across all samples. As shown in Figure (10), the base metal exhibited an average microhardness of 191 HV throughout the sample, indicating a uniform hardness distribution along the building direction. This uniformity suggests consistent microstructural characteristics, which are typically associated with homogeneous and isotropic micro-mechanical properties in the fabricated component [28].

but in (figure 11) the results showed that the average hardness of the weld metal was about (276. 7 HV0.1) As a result of highly distribution of a acicular ferrite phase which is responsible of higher hardness and strength due to its fine, needle-like structure as shown in figure (10) but in in point 2 that the average hardness (255.3 Hv.1) might

have a lower density of acicular ferrite and a higher proportion of bainite or other softer phases. Bainite, while still strong, generally has a lower hardness compared to acicular ferrite. Additionally, the presence of larger grain boundaries or softer inclusions in this region could contribute to the lower hardness. Point. 3 (256.3 Hv.1) the region possibly with a balanced distribution of acicular ferrite and bainite.
During the solidification and cooling process of the weld metal, a large number of Al elements' solid solution in the weld metal results in the reduction of the austenite phase zone which hinders the formation of austenite so that the ferrite formation cannot be fully transformed into austenite in the subsequent cooling process but remains in a coarse skeleton shape in the weld metal structure, thus having an adverse impact on the mechanical properties of the weld metal [29]. Acicular ferrite was higher, the microstructure was finer, and with better impact toughness. [30]. With a rise in heat input, the grain size of the HAZ increased. In figure (13) the microhardness distribution of sample M with different of chemical constituents and due to higher of chrome and carbon inside it which enhanced of composed of carbides during welding so the microhardness measurements as shown in figure increased to reach (242.1Hv.1) .in figure 14 the results showed that The variation in microhardness values may indicate differences in the material's surface properties, testing methodology, or localized heterogeneity in Sample U.
The significant increase at point 4 suggests a potential structural or compositional change as shown in table(6) that enhances hardness at that location. The slight fluctuation between points 1, 2, and 3 could imply minimal variation in the sample's hardness uniformity. The larger increase at point 4 warrants further investigation. Possible reasons could include surface treatment, or impurity concentration [31].

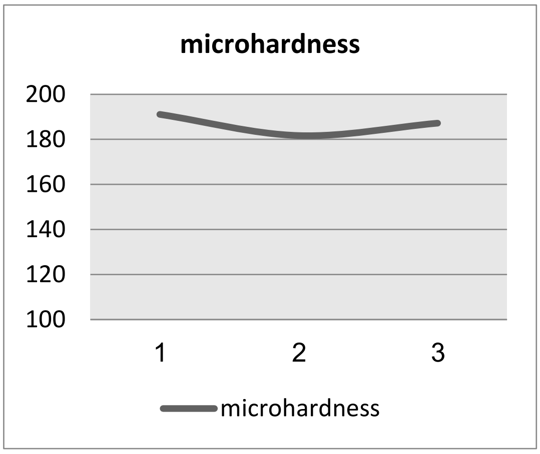

Figure11: Microhardness of Base metal.

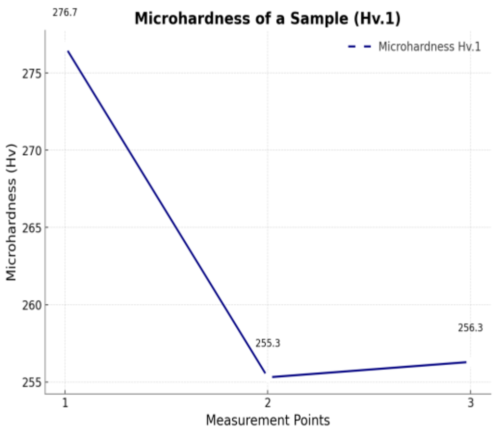

Figure 12: Microhardness of Welded metal.

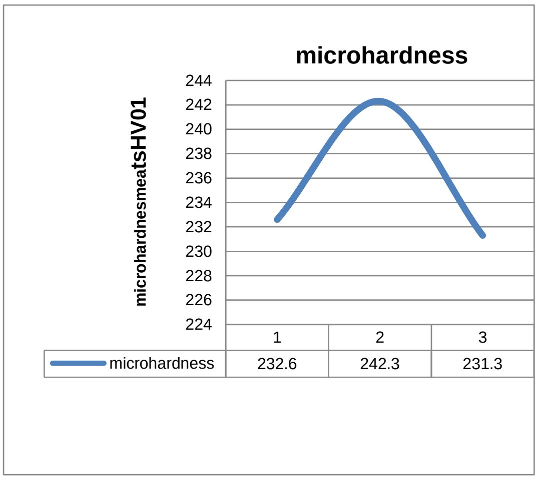

Figure13: Micro hardness of M sample.

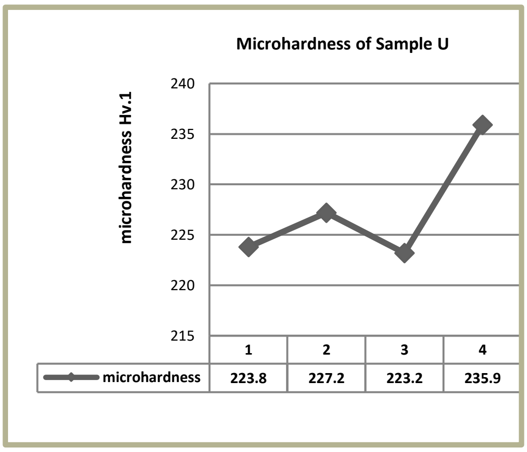

Figure14: Micro hardness of U Sample.

5. Conclusion.

This study addresses the Flux-Cored Arc Welding (FCAW) process, focusing on hard-facing techniques. The E71T-GS electrode wire, compliant with AWS A5.20 standards, was selected for its favorable properties in carbon steel applications.

FCAW was employed as a means for surface hard-facing. Electrode Wire: The E71T-GS wire was chosen due to its excellent impact and wear resistance, making it suitable for hard-facing applications.

• By understanding the microstructure changes induced by FCAW, we can optimize the welding process to enhance the strength hardness, and wear resistance of shredder blades, extending their service life .

•The martensitic microstructure is crucial for the performance and durability of flux cored welded shredder blades. Understanding the crystal structure, transformation mechanisms, and factors influencing martensite formation is key to optimizing the mechanical properties and ensuring the reliable operation of industrial shredding equipment.

• The resulting microhardness can be influenced by the cooling rates and the composition of the filler material used in FCAW [32] this method leverages the unique properties of high-entropy alloys (HEAs) and advanced coatings to achieve superior mechanical characteristics.

• While FCAW is effective for hardening and coating, alternative methods like thermal spraying may also be considered for specific applications, offering different benefits in terms of microstructure and wear resistance.

• Coating Thickness [33]: The resulting coating thickness was approximately 5 mm, which is significant for enhancing wear resistance.

• The use of a flux-cored welding wire with specific alloying agents, such as titanium dioxide and calcium fluoride, enhances the stability of the arc and improves the quality of the coating

• The high hardness and strength of martensite make it an essential material for the fabrication of shredder blades used in industrial waste processing equipment.

• The choice of E71T-GS wire is appropriate for applications requiring good impact and wear resistance, making it ideal for hard-facing purposes

• The results of studies allow us to develop measure to reduce the content of nonmetallic inclusions containing element of fluoride, sodium and aluminum, which in turn can adversely affected the physical and mechanical properties of the clade layer.

• FCAW offers a wide range of filler materials and welding parameters, allowing for controlled microstructure and desired mechanical properties in the weld zone ensuring optimal performance.

• The use of FCAW, combined with through microstructural analysis contributes to the production of reliable and durable welds, reducing the risk of welds failure and ensuring safe operation of shredder blades.

Acknowledgements.

The authors special thank the Libyan Center for Welding Technologies for providing the necessary facilities and resources to carry out the experiments. Special thanks go to **Mr**. **WALEED SALIM MOHAMMED** for his outstanding efforts in performing the welding operations at the Libyan Center for Welding Technologies workshop, which significantly contributed to the completion of this research work.

References

[1] Barnes, D. K., Galgani, F., Thompson, R. C., & Barlaz, M. (2009). Accumulation and fragmentation of plastic debris in global environments. Philosophical Transactions of the Royal Society B: Biological Sciences, 364(1526), 1985-1998.

[2] Sivan, A. (2011). New perspectives in plastic biodegradation. Current Opinion in Biotechnology, 22(3), 422-426.

[3] Chen, H. L., Nath, T. K., Chong, S., Foo, V., Gibbins, C., & Lechner, A. M. (2021). The plastic waste problem in Malaysia: management, recycling and disposal of local and global plastic waste. SN Applied Sciences, 3(4), 1-15.

[4] Thompson, R. C., Moore, C. J., Vom Saal, F. S., & Swan, S. H. (2009). Plastics, the environment and human health: Current consensus and future trends. Philosophical Transactions of the Royal Society B: Biological Sciences, 364(1526), 2153-2166.

[5] United Nations Environment Programme. (2018). UNEP Report on Single-Use Plastics.

[6] Santander, P., Sanchez, F. A. C., Boudaoud, H., & Camargo, M. (2020). Closed-loop supply chain network for local and distributed plastic recycling for 3D printing: A MILP-based optimization approach. Resources, Conservation and Recycling, 154, 104531.

[7] D’Ambrières, W. (2019). Plastics recycling worldwide: current overview and desirable changes. Field Actions Science Reports, Special Issue 19, 12-21.

[8] Kreiger, M. A., Mulder, M., Glover, A. G., & Pearce, J. M. (2014). Life cycle analysis of distributed recycling of post-consumer high-density polyethylene for 3D printing filament. Journal of Cleaner Production, 70, 90-96.

[9] Sea Communities. (2020). Plastic for Profit. Retrieved from https://seacommunities.com/plastic-profit
[10]] Precious Plastic Universe. (2020). Precious Plastic. Retrieved from https://preciousplastic.com/
[11] Prabanjan, K. S., Karthick, J., Kumar, S. R., Ramkumar, A., & Riswan, A. (2020). Wear behavior and metallurgical characteristics of particle reinforced metal matrix composites produced by hard-facing: A review. Materials Today: Proceedings. In press. [CrossRef].
[12] [Nagentrau, M., Tobi, A. M., Sambu, M., & Jamian, S. (2019). The influence of welding condition on the microstructure of WC hard-facing coating on carbon steel substrate. International Journal of Refractory Metals and Hard Materials, 82, 43-57. [CrossRef].
[13] Dilawary, S. A. A., Motallebzadeh, A., Atar, E., & Cimenoglu, H. (2018). Influence of Mo on the high temperature wear performance of NiCrBSi hard-facings. Tribology International, 127, 288-295. [CrossRef].
[14] Mohamat, S. A., Ibrahim, I. A., Amir, A., & Ghalib, A. (2012). The effect of flux core arc welding (FCAW) processes on different parameters. Procedia Engineering, 41, 1497-1501. https://doi.org/10.1016/j.proeng.2012.07.341
[15] Tavares, S. S., Souza, R. P. D., & da Silva, F. A. V. (2016). Influence of manganese content on the microstructure and mechanical properties of austenitic steels. Journal of Materials Science, 51(1), 1-14.
[16] Giambattista, J. E. (2013). Optimizing welding parameters to improve weld quality. Welding Journal, 92(2), 67-72.
[17] Zhang, Y. A. O., & Zhang, Y. (2011). The effect of preheating on the mechanical properties of welded joints. Welding International, 25(3), 206-213.
[18] Andrić, R. S., & Hu, O. H. (2012). Impact of preheating on the microstructure of welded joints. Materials Science and Engineering: A, 513-514, 165-171.
[19] Prasad, K. R. A. A. B. D. H. (2008). Effects of cooling rate on the microstructure and hardness of welds. Welding Research Supplement, 87(8), 98s-104s.
[20] Lee, H. J., & Lee, H. (2015). Effect of Cr content on microstructure and mechanical properties of low carbon steel welds. International Journal of Electronics and Science, 10, 8028-8040.
[21] []21] Zhang, X., Li, M., & Wu, Z. (2018). Investigating the microstructure and mechanical properties of flux-cored arc welds. Journal of Materials Processing Technology, 257, 124-131.
[22] Chen, H., Liu, Y., & Wang, T. (2019). Effect of shielding gas composition on the quality of FCAW welds. International Journal of Welding and Joining, 34(2), 89-95.
[23] Yan, J., Zhao, Q., & Lee, K. (2020). Thermal analysis and heat input control in flux-cored arc welding. Welding Journal, 99(7), 56-64.
[24] Song, F., Yin, C., Hu, F., & Wu, K. (2022). Effects of Mn-depleted zone formation on acicular ferrite transformation in weld metals under high heat input welding. Materials, 15, 8477. https://doi.org/10.3390/ma1518477
[25] Srikarun, B., Oo, H. Z., & Muangjunburee, P. (2021). Influence of different welding processes on microstructure, hardness, and wear behavior of martensitic hardfaced cladding. Journal of Materials Engineering and Performance, 30(12), 8984-8995. https://doi.org/10.1007/s11665-021-06109-0
[26] Tippayasam, C., Taengwa, C., Palomas, J., Siripongsakul, T., Thaweechai, T., & Kaewvilai, A. (2020). Effects of flux-cored arc welding technology on microstructure and wear resistance of Fe-Cr-C hard-facing alloy. Materials Today: Communications, 35, 105569. https://doi.org/10.1016/j.mtcomm.2023.105569
[27]]Ozkana, E. (2024). Investigation of the alloying elements effect in the flux-cored wire and submerged arc welding flux combination. Journal of Materials Today Communications, 35, 105569. https://doi.org/10.1016/j.mtcomm.2023.105569
[28] Sridharan, N., Noakes, M. W., Nycz, A., et al. (2018). On the toughness scatter in low alloy C-Mn steel samples fabricated using wire arc additive manufacturing. Materials Science and Engineering: A, 713, 18-27. https://doi.org/10.1016/j.msea.2017.11.101
[29] Ricks, R. A., Howell, P. R., & Barritte, G. S. (2020). The nature of acicular ferrite in HSLA steel weld metals. Journal of Materials Science and Engineering, 15(6), 165-171.
[30] Oktadinata, H., Winarto, W., & Siradj, E. S. (2020). Microstructure and impact toughness of flux-cored arc welded SM570-TMC steel at low and high heat input. Materials Science Forum, 991, 3-9. https://doi.org/10.1016/j.msf.2020.991
[31] Z., Hu, F., Li, Y., Lin, S., & Cai, X. (2022). Microstructure and mechanical properties of the ternary gas shielded narrow-gap GMA welded joint of high-strength steel. Crystals, 12, 1566. https://doi.org/10.3390/cryst12121566
[32] Wen, C., Wang, Z., Deng, X., & Misra, R. D. K. (2018). Effect of heat input on the microstructure and mechanical properties of low alloy ultra-high strength structural steel welded joint. Steel Research International, 89, 1700500. https://doi.org/10.1002/srin.201700500
[33] Sharma, P., & Kumar, S. (2019). "A Comparative Study on Flux-Cored Arc Welding (FCAW) and Other Welding Techniques in Structural Steel Applications." International Journal of Mechanical Engineering and Technology (IJMET), 10(3).